Available online www.jsaer.com

***Journal of Scientific and Engineering Research*, 2018, 5(1):184-196**

Research Article

ISSN: 2394-2630
CODEN(USA): JSERBR

Effect of Stratification on Homogeneous Sheared Turbulence through Second Order Model

Saida NAIFER[1], Mounir BOUZAIANE[2]

[1]Laboratory of Physics of Fluids, Physics Department, Faculty of Science of Tunis University of Tunis El-Manar,2092 El Manar 2, Tunis, Tunisia

[2]Department of Physics, Faculty of Sciences of Bizerte, Zarzouna, Banzart 7021, Tunisia

Abstract The aim of this work is the study of the effect of stratification on homogeneous sheared turbulence through a second order modeling. The Gibson-Launder model is retained for modeling the time evolution equations either for the kinematic and scalar fields. The asymptotic behavior of the dimensionless kinematic and scalar parameters is numerically studied. Governing equations are castled in dimensionless form by introducing components b_{ij} of the anisotropic tensor of Reynolds for kinematic field and the components F_i of dimensionless scalar flux. A numerical approach consists on integrating non linear system of seven differential equations using the fourth order Runge-Kutta method. The gradient Richardson number R_i is used to describe the importance of stratification on turbulence evolution. The results of the Direct Numerical Simulation of Jacobitz and other numerical second order models are retained for comparing with the obtained results. Through numerical approach, asymptotic behavior of the principal component b_{12} of anisotropy as function of stratification has been observed. The evolution of the non dimensional anisotropy b_{11} is affected by stratification. The nondimensional scalar flux F_1 is greatly affected on the Richardson number R_i.

Keywords Turbulence modeling, Gibson Launder model, Stable stratification, Equilibrium states

1. Introduction

Turbulence is a problem often of importance in atmosphere and in many Engineering applications. Perhaps geophysical and turbomachinery are among the principal turbulent flows dominated by stratification effect [1]. The effect of body forces associated with density stratification is important in a wide variety of turbulent flows. Thus, it has been the subject of a numerous experimental and numerical investigations.

The turbulence of classical fluids is an everyday phenomenon, which can be readily observed in the flow of a stream or river. Recent experiments and numerical simulations have coordinated highlighting between turbulence in quantum fluids and turbulence in ordinary fluids (classical turbulence) [2]. The term quantum turbulence denotes the turbulent motion of quantum fluids, systems such as superfluid helium and atomic Bose-Einstein Condensates [3]. Thus in classical fluid turbulence, energy is dissipated through viscosity.

Stratified flows are found widely in the ocean, atmospheric boundary layers, and some lakes and rivers on the lands. They are one of the most important flows in the geophysical research. Owing to the increasing interest in environmental problems, the case with pure stratification has been reported by numerical approach [4, 5] and experimental studies [6, 7].

Occurring to many experimental difficulties, numerical approaches seem to be the principal direction of investigation for turbulence researches. Recently, second order models have been used by Khaleghi et al [8] to study complex configurations of turbulent flows. Bouzaiane et al [9] have also used numerical approaches to

study the effect of stratification in homogeneous sheared turbulence. The effect of the dimensionless gradient Richardson number R_i on stratification was widely analyzed by Rohr et al [10].

A numerical study of this flow was investigated by Susan Friedlander [11] and Howard et al [12]. Surrounded by the first-class foremost laboratory experiments are those of Piccirillo and Van Atta [13] and Rohr et al [14]. On the understudy assign, numerical simulations of such flows have been performed by Gerz et al [15], Holt et al [16], Kaltenbach [17], Jacobitz et al [18], Jacobitz and Sarkar [19-21], Jacobitz [22, 23]. In actuality, equilibrium states of several examples of homogeneous shear flows have been used in the analysis of turbulence second order models (Speziale et al) [24, 25].

The principal objective of this work is to predict asymptotic equilibrium states in homogeneous turbulence submitted to stratification using Gibson-Launder second order models. The work is structured as follows. We begin in section 2 by presenting general equation of homogeneous sheared turbulence. In section 3, Gibson-Launder second order model is presented and the evolution equations are modeled. Section 4 is dedicated to numerical integration of dimensionless transport equations. The obtained results are analyzed and discussed in section 5. A conclusion makes the last part of this work.

Nomenclature

b_{ij}	Reynolds stress anisotropy tensor
e_{imp}	component of permutation tensor
g_i	gravitational acceleration ($m.s^{-2}$)
K	turbulent kinetic energy ($m^2.s^{-2}$)
P	terms of production due to mean kinematic and scalar gradients
p	pressure ($N.m^{-2}$)
p'	fluctuation of the pressure ($N.m^{-2}$)
R_i	dimensionless Richardson number
S	shear rate (s^{-1})
S_{ij}	mean rate of strain (s^{-1})
S_T	mean scalar gradient ($°C.m^{-1}$)
T	temperature (°C)
u_i'	i-th component of the fluctuating velocity ($m.s^{-1}$)
$\overline{U_i}$	i-th component of mean velocity ($m.s^{-1}$)
$\overline{u_i'u_j'}$	Reynolds stress tensor ($m^2.s^{-2}$)
$\overline{u_i'\theta}$	turbulent scalar flux ($m°C.s^{-1}$)
W_{ij}	mean vorticity tensor (s^{-1})
x_i	component of an orthonormal Cartesian coordinate system (m)

Greek Symbols

α	thermal diffusivity of fluid ($m^2.s^{-1}$)
β	thermal expansion coefficient (K^{-2})
δ_{ij}	Kronecker Symbol
ε	terms of dissipation due to molecular effects ($m^2.s^{-3}$)
τ	non dimensional time
θ	fluctuation of the scalar (°C)
$\overline{\theta^2}$	temperature variance ($°C^2$)
μ	dynamic viscosity ($kg.m^{-1}.s^{-1}$)

ν	kinematic viscosity ($m^2.s^{-1}$)
ρ_0	reference density of the fluid ($kg.m^{-3}$)
Φ_{ij}	terms of pressure-strain correlation ($m^2.s^{-3}$)
$\Phi_{i\theta}$	terms of pressure-temperature gradient correlation ($°C.m.s^{-2}$)

2. Mathematical Consideration

A stratified homogeneous shear flow of an incompressible fluid in a rotating system is considered in this work. The velocity $\overline{U} = \left(\overline{U_1}, 0, 0\right)$ is according to x_1 and has a constant gradient $S = \partial\overline{U_1}/\partial x_2$ according to x_2. A scalar field, with a constant mean gradient $S_T = \partial T/\partial x_2$ according to x_2.

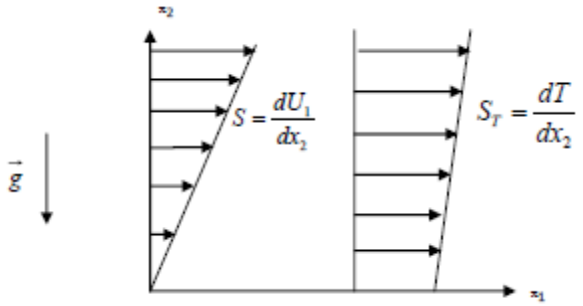

Figure 1: Draft according to stratified homogeneous turbulent flow

From the basic equation of continuity, momentum and energy conservation equations, for a steady state incompressible turbulent flow [26, 27], the transport equations for the components $\overline{u_i'u_j'}$, $\overline{u_i'\theta}$, K and $\overline{\theta^2}$ describing the considered flow are derived and given by :

$$\frac{d}{dt}\left(\overline{u_i'u_j'}\right) = P_{ij} + G_{ij} + \Phi_{ij} - \varepsilon_{ij} \tag{1}$$

Here $\frac{d}{dt} = \frac{\partial}{\partial t} + \overline{U_k}\frac{\partial}{\partial x_k}$ is the total time derivative.

$$\frac{d}{dt}\left(\overline{u_i'\theta}\right) = P_{i\theta} + G_{i\theta} + \Phi_{i\theta} - \varepsilon_{i\theta} \tag{2}$$

If we contract the indices i and j in Eq.1 [28], then we obtain:

$$\frac{dK}{dt} = P + G - \varepsilon \tag{3}$$

Where $K = \frac{1}{2}\overline{u_i'u_i'}$

$$\frac{d}{dt}\left(\overline{\theta^2}\right) = 2\left(P_\theta - \varepsilon_\theta\right) \tag{4}$$

With the goal of obtaining a closed system of differential equations, the turbulence modeling remains an important approach retained by several authors [27]. The second order modeling is retained here and consists to model the pressure-strain and pressure-temperature gradient correlations. The Gibson and Launder (GL) model is retained here for these terms which are written in the following forms:

$$\Phi_{ij} = -c_1\, b_{ij}\varepsilon + c_2\, KS_{ij} + c_3\, K\left(b_{ik}S_{kj} + b_{jk}S_{ki} - \frac{2}{3}b_{mn}S_{mn}\delta_{ij}\right) + c_4\, K\left(b_{ik}W_{jk} + b_{jk}W_{ik}\right) - c_5\left(G_{ij} - \frac{1}{3}G_{kk}\delta_{ij}\right). \tag{5}$$

$$\Phi_{i\theta} = -c_{\theta 1}\frac{\varepsilon}{k}\overline{u_i'\theta} + (c_{\theta 2}+c_{\theta 3})\overline{u_k'\theta}\,S_{ik} + (c_{\theta 2}-c_{\theta 3})\overline{u_k'\theta}\,W_{ik} + c_{\theta 4}\,\overline{u_i'u_k'}\frac{\partial \overline{T}}{\partial x_k} + c_{\theta 5}\,\beta\,\overline{\theta^2}\,g_i\,. \quad (6)$$

$$\frac{d\varepsilon}{dt} = c_{\varepsilon 1}\frac{\varepsilon(P+G)}{K} - c_{\varepsilon 2}\frac{\varepsilon^2}{K} - c_{\varepsilon 3}\beta_i\frac{\varepsilon}{K}\overline{u_i'\theta}\,. \quad (7)$$

$$\varepsilon_\theta = \frac{\overline{\theta^2}}{r}.\frac{\varepsilon}{K}\,. \quad (8)$$

Where C_i , $C_{\varepsilon i}$ and $C_{\theta i}$ are the numerical constants of model:

$c_1 = 3.6$, $c_2 = 0.8$, $c_3 = c_4 = 1.2$, $c_5 = 0.5$, $c_{\varepsilon 1} = 1.45$, $c_{\varepsilon 2} = 1.9$, $c_{\varepsilon 3} = 1.0$, $c_{\theta 1} = 3$, $c_{\theta 2} = 0.33$ $c_{\theta 3} = c_{\theta 4} = 0$, $c_{\theta 5} = 0.33$ and $r = 0.8$.

With the purpose of acquisition the dimensionless equations, basic equations (1)-(4) and (7) are deposited in dimensionless form by laying on the dimensionless time $\tau = St$, the kinematic components $b_{ij} = \left(\overline{u_i'\,u_j'}/2K\right) - \left(\delta_{ij}/3\right)$ [29] and $\left(\varepsilon/SK\right)$[20], and the scalar component $F_i = \left(g/\rho_0\right)\left(\overline{u_i'\theta}/KS\right)$ and $F_\theta = \left(g\beta/S\right)^2\left(\overline{\theta^2}/K\right)$ [30].

$$\frac{dK^*}{d\tau} = -\left(2b_{12} + \frac{\varepsilon}{SK} - F_2\right)K^*\,. \quad (9)$$

$$\frac{d(b_{ij})}{d\tau} = -\left(\frac{C_1}{2} - 1 + \frac{P+G}{\varepsilon}\right)\left(\frac{\varepsilon}{SK}\right)b_{ij} + \left(\frac{C_3-2}{2}\right)\left(b_{ik}S^*_{jk} + b_{jk}S^*_{ik} - \frac{2}{3}b_{mn}S^*_{mn}\delta_{ij}\right) + \left(\frac{C_4-2}{2}\right)\left(b_{ik}W^*_{jk} + b_{jk}W^*_{ik}\right) + \left(\frac{C_2}{2} - \frac{2}{3}\right)S^*_{ij} - \left(\frac{C_5-1}{2}\right)\left(F_i\delta_{j2} + F_j\delta_{i2} - \frac{2}{3}F_k\delta_{k2}\delta_{ij}\right). \quad (10)$$

$$\frac{d}{d\tau}\left(\frac{\varepsilon}{SK}\right) = \left[(C_{\varepsilon 1}-1)\left(\frac{P+G}{\varepsilon}\right) - (C_{\varepsilon 2}-1) - c_{\varepsilon 3}\frac{\beta_i}{\varepsilon}\overline{u_i'\theta}\right]\left(\frac{\varepsilon}{SK}\right)^2. \quad (11)$$

$$\frac{d\,F_i}{d\,\tau} = 2\left(C_{\theta 4}-1\right)\left(b_{ik} + \frac{\delta_{ik}}{3}\right)R_i\,\delta_{k2} + \left(1-C_{\theta 5}\right)F_\theta\,\delta_{i2} + \left(C_{\theta 2}+C_{\theta 3}-1\right)\times\left(\delta_{i1}\,\delta_{k2} + \delta_{i2}\delta_{k1}\right)\left(\frac{F_k}{2}\right) + \left(C_{\theta 2}-C_{\theta 3}-1\right)\times\left(\delta_{i1}\,\delta_{k2} - \delta_{i2}\delta_{k1}\right)\left(\frac{F_k}{2}\right) - \left(C_{\theta 1}-1+\frac{P+G}{\varepsilon}\right)\left(\frac{\varepsilon}{S\,K}\right)F_i\,. \quad (12)$$

$$\frac{dF_\theta}{d\tau} = -2R_iF_k\delta_{k2} - \left(\frac{P+G}{\varepsilon} - 1 + 2r\right)\left(\frac{\varepsilon}{SK}\right)F_\theta\,. \quad (13)$$

Where $R_i = g\,\beta\,S_T/S^2$ is the gradient Richardson number.

The dimensionless quantities are:

$\tau = St$, $K^* = K/K_0$, $S^*_{ij} = S_{ij}/S$, $W^*_{ij} = W_{ij}/S$, $F_i = (g\beta/KS)\overline{u_i'\theta}$ and $F_\theta = (g\beta/S)^2\left(\overline{\theta^2}/K\right)$. (14)

At this step, a numerical integration of the differential equations is started. Obtained results will be discussed in the following sections.

3. Numerical Integration and Results

3.1. Asymptotic Equilibrium States

Study of asymptotic equilibrium states in homogeneous sheared turbulence has been essentially developed by Speziale and Mhuiris [31] to evaluate several second order models of Φ_{ij} and time evolution equation of

dissipation rate [32, 33]. More recently, authors are interested in predictions of equilibrium states in homogeneous sheared turbulence affected by stratification [34, 35]. However, to our knowledge, no previous work is interested in the prediction of equilibrium states by the Gibson Launder second order models. This creates the aim of this part of our work.

A fourth order Runge-Kutta method is retained for the numerical integration of differential non-linear system submitted to the initial condition of the direct numerical simulation of Jacobitz [23]. At long time evolution, the dimensionless parameters reach asymptotic equilibrium values noted respectively:

$(b_{11})_\infty$, $(b_{22})_\infty$, $(b_{12})_\infty$, $(\varepsilon/SK)_\infty$, K/K_0, $(F_1)_\infty$, $(F_2)_\infty$, $(F_\theta)_\infty$.

Table 1 and table 2 give a summary of the asymptotic equilibrium states for dimensionless kinematic and scalar parameters.

Table 1: Equilibrium values predicted for kinematic parameters

R_i	**0**	**0.1**	**0.2**	**0.5**	**0.6**
$(b_{11})_\infty$	0.344	0.341	0.337	0.323	0.317
$(b_{22})_\infty$	0.089	0.091	0.092	0.101	0.104
$(b_{12})_\infty$	-0.153	-0.144	-0.135	-0.108	-0.098
$(\varepsilon/SK)_\infty$	0.278	0.264	0.249	0.207	0.194

Table 2: Asymptotic equilibrium states of scalar parameters

R_i	**0**	**0.1**	**0.2**	**0.5**	**0.6**
$(F_1)_\infty$	0.0196	0.075	0.130	0.281	0.326
$(F_\theta)_\infty$	-0.0392	0.052	0.145	0.441	0.546

It is necessary here to mark that asymptotic equilibrium values obtained by GL model for the kinematic field are functions of the Richardson number R_i.

Asymptotic equilibrium states have been reached for several values of R_i. We show that the equilibrium values $(b_{11})_\infty$ and $(\varepsilon/SK)_\infty$ decrease when R_i increases, whereas the equilibrium values $(b_{22})_\infty$ and $(b_{12})_\infty$ increase with the increase of Richardson number R_i. From Table 2, we note that stratification affects not only the kinematic fields but also the scalar field. We remark that the asymptotic equilibrium values of scalar dimensionless parameters change with R_i. The equilibrium values $(F_1)_\infty$ and $(F_\theta)_\infty$ increase with the increase of R_i from 0 to 0.6.

The effect of several parameters such as the gradient Richardson number R_i on turbulence evolution will be studied on the next section of our work.

The effect of Richardson number is firstly studied on the following subsection.

3.2. Influence of the Richardson number on kinematic fields

Now, dimensionless kinematics and scalar parameters versus dimensionless time (growing to 200) are presented for the values $R_i = 0.1$, $R_i = 0.6$, $R_i = 1$ and $R_i = 2$.

In figure 2, time evolutions of the dimensionless shear number (ε/SK) according to dimensionless time τ and for different gradient Richardson number R_i are exhibited. A fast decrease observed for a dimensionless time τ less than 20, which is followed by a slight increase for $R_i = 0$, $R_i = 0.1$ and $R_i = 0.6$ and a rapid tendency to equilibrium states at $\tau = 100$ for the two first values of R_i.

For $R_i = 1$ and $R_i = 2$ and for $\tau > 20$, the dimensionless number (ε/SK) continues to decrease without reaching asymptotic equilibrium states for $\tau < 200$. However, general tendency to asymptotic equilibrium values $(\varepsilon/SK)_\infty$ for $\tau < 200$ only in the case $R_i = 0$ and $R_i = 0.1$ is obtained.

In these cases, asymptotic equilibrium states are reached for $\tau \approx 100$. The asymptotic value $(\varepsilon/SK)_\infty$ decreases strongly when the gradient Richardson number R_i is increased as presented on the previous tables.

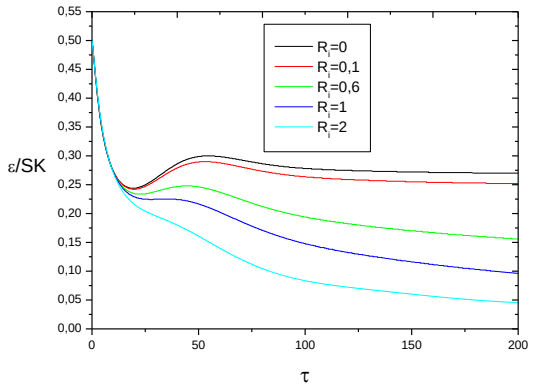

Figure 2: Time evolution of (ε/SK) for several values of R_i.

Now, a comparison between our obtained results and those obtained by several models will be proposed.

In figure 3, time evolution of non dimensional shear number (ε/SK) according to the three models of Gibson Launder (GL) [36], Craft and Launder (CL) [28] and Shih and Lumley (SL) [37] models in the case $R_i = 0.6$ of Richardson number are displayed. We note that the best agreement between the prediction of the GL model and the values of CL model as well as SL model is observed for the value of $(\varepsilon/SK)_\infty$ for $\tau < 50$.

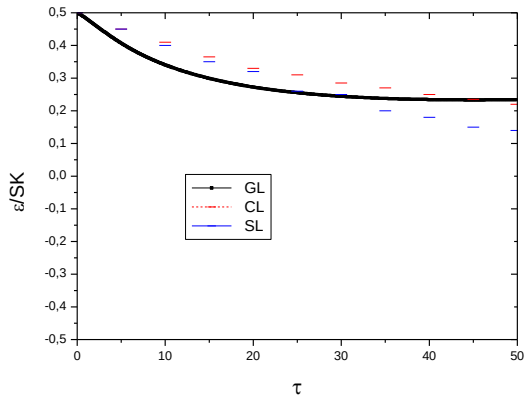

Figure 3: Time evolution of (ε/SK) for three models for $R_i = 0.6$.

Figure 4 shows time evolution of (ε/SK) according to two models of Launder Reece Rodi (LRR) [38] and GL models for the value $R_i = 0.2$ of Richardson number. On this figure, an asymptotic equilibrium behavior is observed for both models.

The result presented is in contradiction with the result of LRR model. No agreement between predictions of GL model and values of LRR model has been observed for the value 0.2 of R_i for dimensionless time τ less than 50.

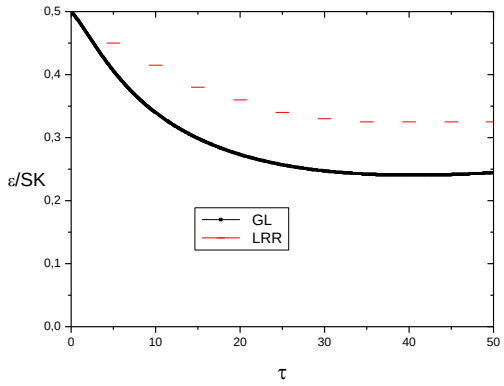

Figure 4: Time evolution of (ε/SK) *for two models in the case* $R_i = 0.2$.

Figure 5 shows time evolution of the component of anisotropy b_{11} for several values of gradient Richardson number R_i. A fast decrease is observed for $\tau < 10$, which is followed by a strong growth in the cases $R_i = 0$, $R_i = 0.1$ and $R_i = 0.6$.

A moderate growth is observed for $\tau > 10$ in the case $R_i = 1$ and a weak growth of b_{11} is observed in the case $R_i = 2$. In fact, the equilibrium values predicted for b_{11} have been observed for R_i in the larger interval $0 \le R_i \le 2$. Asymptotic equilibrium states are reached at $\tau = 60$ and for $0 \le R_i \le 1$. We note that the equilibrium value is reached for $R_i = 0.1$ more quickly than the case of $R_i = 2$.

The same asymptotic equilibrium behavior is also observed for each value of Richardson number between 0 and 1. The equilibrium value of anisotropy b_{11} decreases with increasing Richardson number R_i from 0 to 2.

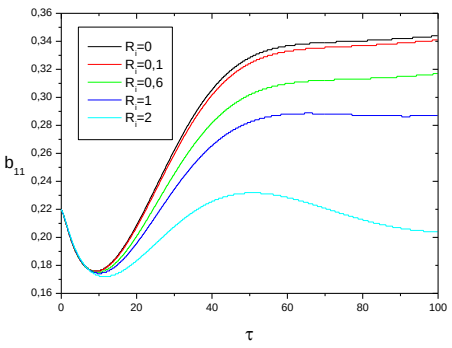

Figure 5: Time evolution of b_{11} *according to* R_i .

Figure 6 shows time evolution of the component of anisotropy b_{11} according to GL model as function of R_i. In comparison to values of the DNS data of Jacobitz [18] for which asymptotic equilibrium states are obtained for different values of the Richardson number R_i. In Figure 6, a good agreement between the prediction of the GL model and the values of DNS data of Jacobitz is observed for the value of (b_{11}) for $0.2 < R_i < 0.5$.

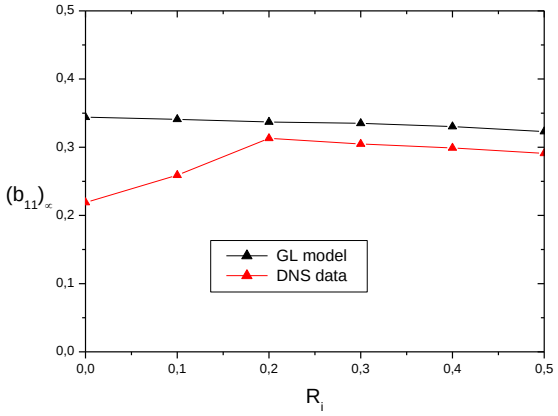

Figure 6: Evolution of $(b_{11})_{\infty}$ *as function of* R_i

In Figure 7, time evolutions of the component of anisotropy b_{22} for five different values of the gradient Richardson number R_i are displayed. A steady evolution of b_{22} for $\tau < 8$, which is followed by a strong decrease to reach asymptotic equilibrium states has been observed. We note that the asymptotic equilibrium state $(b_{22})_{\infty}$ for $R_i = 2$ is reached more quickly at $\tau = 125$ than in the case of weak stratification ($R_i = 0.1$) which predicts an equilibrium state at $\tau = 150$.

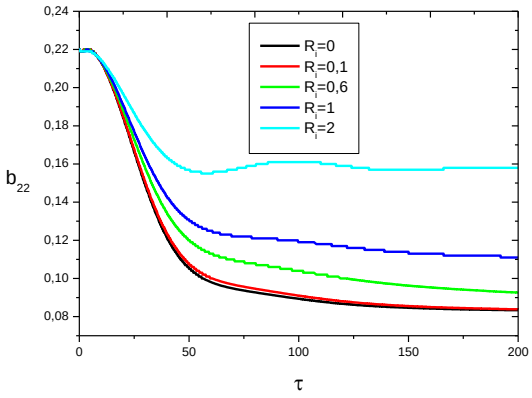

Figure 7 Time evolution of b_{22} *for several values of* R_i

Figure 8 shows the evolution of the principal component of anisotropy b_{12} obtained by GL model for different values of the gradient Richardson number as a function of the dimensionless time $\tau = St$.

A fast decrease, for $\tau < 40$, which reaches a minimum moving to the left as the Richardson number R_i increases. The evolution of b_{12} for $\tau > 40$ is followed by a slight increase to reach the asymptotic equilibrium states. This evolution confirms the existence of asymptotic equilibrium states for the component b_{12} in the case $R_i = 0$ and $R_i = 0.1$. It also indicates that $(b_{12})_{\infty}$ grows with R_i growing from neutral stratification $(R_i = 0)$ to strong stratification $(R_i = 2)$. This result is in concordance with our previous results [9]. The equilibrium value is achieved in the cases $R_i = 0$ and $R_i = 0.1$ more quickly than the case of $R_i = 2$.

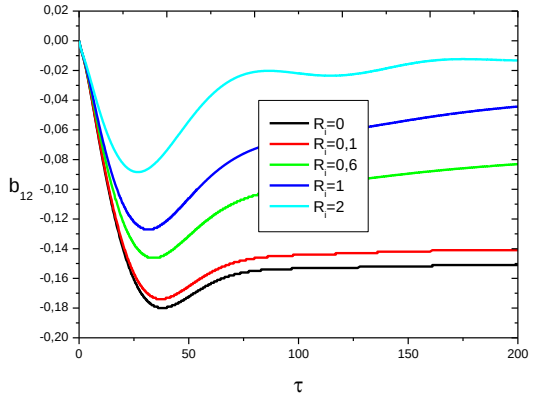

Figure 8: Time evolution of b_{12} in different cases of R_i

Figure 9 shows time evolution of the component of anisotropy b_{12} according to the GL model for the case $R_i = 0.2$ of Richardson number for an intermediate band of τ, in the range $[0, 50]$. In this figure, the GL model shows a good agreement with the asymptotic value of the component of anisotropy $(b_{12})_\infty$ of DNS data of Jacobitz for the value $R_i = 0.2$ of the Richardson number when τ is greater than 30. The equilibrium state is achieved for a low non dimensional time $\tau = 10$ for DNS data of Jacobitz.

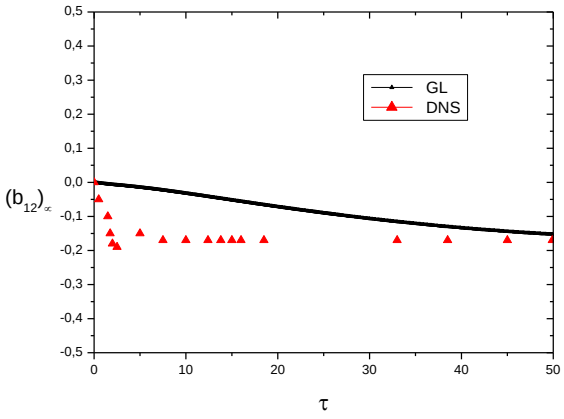

Figure 9: Time evolution of $(b_{12})_\infty$ for two models for $R_i = 0.2$.

Table 3 summarizes the asymptotic equilibrium values obtained by several models for the case of neutral stratification.

We see that the GL model indicates the best agreement with the prediction of Speziale Sarkar and Gatski (SSG) [39], Rotta-Kolmogorov (RK) [40], Large-Eddy Simulations (LES) [41], Fu,Launder and Tselepidakis (FLT) [42] models, in comparison with the Launder Reece and Rodi (LRR) model [38], for the asymptotic value of the component of anisotropy $(b_{12})_\infty$.

Table 3: Equilibrium values predicted for b12 parameter for different models

Equilibrium value	GL model	LRR model	SSG model	RK model	LES model	FLT model
$(b_{12})_\infty$	-0.153	-0.185	-0.156	-0.169	-0.15	-0.144

3.3. Influence of the Richardson number on scalar field

Stratification affects not only the kinematic fields but also the scalar field. It is the turbulent flux rate F_i that is the most one affected by the stratification effects. Then the evolution of dimensionless rates for the scalar field is explained.

Figure 10 shows the influence of gradient Richardson number on F_1. A weak increase observed for $\tau < 5$, which is followed by a slight decrease for $R_i = 2$ and a moderate decrease for the other cases of R_i to reach a minimum. Then a fast increase is observed and a rapid tendency to equilibrium states at $\tau = 50$ for the four first values $R_i = 0$, $R_i = 0.1$, $R_i = 0.6$ and $R_i = 1$. For $R_i = 2$, $(F_1)_\infty$ is reached for $\tau > 90$. Hence stratification has a great effect on the non dimensional turbulent flux F_1. The asymptotic equilibrium value of the turbulent flux rate F_1 increases with the increase of the Richardson number R_i.

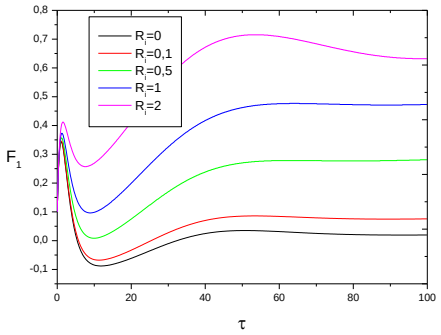

Figure 10: Time evolution of F_1 for different values of R_i.

The time evolution of F_θ is shown on Figure 11 for different values of Richardson number R_i. The values of F_θ decrease to a minimum at $\tau = 10$ after a slight increase and then increase to achieve the equilibrium state. A general tendency to asymptotic equilibrium behavior is also observed for each value of R_i. The asymptotic equilibrium values increase with increasing Richardson number. This result is coherent with the physical phenomena. A growth of scalar gradient conducts to an increase of the scalar variance.

Asymptotic equilibrium states have been obtained for different cases. Essentially for $R_i = 1$ of the Richardson number, an equilibrium states are quickly reached.

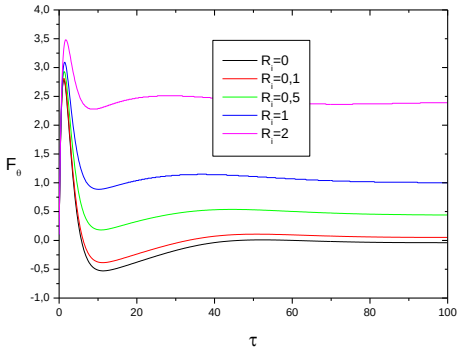

Figure 11: Time evolution of F_θ as function of R_i.

4. Conclusion

A turbulent shear flow submitted to stratification is studied through the Gibson-Launder second order model.

The study of asymptotic equilibrium states of dimensionless parameters was the principal objective of this work. The dimensionless evolution equations of kinematic and scalar parameters are written and integrated using the fourth order Runge-Kutta method.

The first part of this work is dedicated to the general transport equation of turbulent parameters. It is followed by the modeling of transport equations by the GL second order model and it is justified that non dimensional parameters can substitute the turbulent parameters for the kinematic and scalar fields.
The main results obtained from this study can be summarized as follows:
The Gibson Launder model is one of the most commonly used ensuring the closure of the evolution equation of the kinematic field and the scalar field.

- The GL model predicts time evolution of kinematic and scalar fields for the stratified homogeneous shear. The asymptotic equilibrium values obtained for (ε/SK), b_{11}, b_{22} and b_{12} are seriously affected by several values of the gradient Richardson number R_i. We also add that stratification has a great effect on nondimensional turbulent flux F_1 and F_θ.

- For the influence of R_i on equilibrium state of (ε/SK), the best agreement between the results of the three models of GL, CL and SL is obtained. However, no agreement between predictions of GL models and values of LRR model has been observed.

- In comparison to values of the DNS data of Jacobitz, a qualitative agreement is observed for the values of equilibrium state of b_{11} and b_{22} obtained using the GL model.

- Asymptotic equilibrium behavior of dimensionless kinematic and scalar parameters depends on the stratification through the gradient Richardson number R_i. The effect of variation of R_i on the time evolution of the kinematic and scalar dimensionless parameters is observed.

- The stratification effects dominate the evolution of (ε/SK), b_{12} and F_1.

- The evolution of the non dimensional anisotropy b_{11} is affected by the stratification.

To improve prediction of GL model taking into account effect of stratification, corrections can be introduced in model coefficient. The study of the analogy of rotation effect and stratification effect through dimensionless parameters R_i and (Ω/S) can also make an extension of this work and be an interesting future investigation.

References

[1]. Mazaheri. K., N, Chaharlang Kiani. K., Karimi. M., (2017) A modified turbulent heat-flux model for predicting heat transfer in separating-reattaching flows and film cooling applications, Applied Thermal Engineering, vol. 110, pp. 1609-1623.
[2]. Skrbek. J., and Sreenivasan. K. R., (2012) Developed quantum turbulence and its decay, Physics of Fluids, vol. 24, pp. 011301.
[3]. Skrbek, L., (2011) Quantum turbulence. Journal of Physics: 13th European Turbulence Conference (ETC13).
[4]. Herring. J. R., Q Métais. O., (1989) Numerical experiments in forced stably stratified turbulence, Journal of Fluid Mechanics, vol. 202, pp. 97-115.
[5]. Smith. M. L., and Waleffe. F., (2002) Generation of slow large scales in forced rotating stratified turbulence, Journal of Fluid Mechanics, vol. 451, pp. 145-168.
[6]. Fincham. A. M., Maxworthy. T., and Spedding. G. R., (1996) Energy dissipation and vortex structure in freely-decaying, stratified grid turbulence, Dynamics of Atmospheres and Oceans, Vol. 23, pp. 155-169.
[7]. Praud. O., Sommeria. J., Fincham. A. M., (2006) Decaying grid turbulence in a rotating stratified fluid, Journal of Fluid Mechanics, Cambridge University Press (CUP), vol. 547, pp. 389-412.
[8]. Khaleghi. E., Lin. Y.-S., Meyers. M. A., & Olevsky. E.A., (2010) Spark plasma sintering of Tantalum carbide. Scripta Materialia, vol. 63, Issue. 6, pp. 577-580.
[9]. Bouzaiane. M., Ben Abdallah. H., and Lili. T., (2003) A stably on the asymptotic behaviors of dimensionneless parameters in a stably homogeneous sheared turbulence. Journal of turbulence, Volume 4, Issue 1, pp. 002.

[10]. Rohr. J. J., Itsweire. E. C., Helland. K. N., Van Atta. C. W., (1988a) Growth and decay of turbulence in a stably stratified shear flow, Journal of Fluid Mechanics, vol.195, pp 65-77.
[11]. Susan Friedlander (1976), Quasi-steady flows of a rotating stratified fluid in a sphere, Journal of Fluid Mechanics, vol.76, pp. 209-228.
[12]. Howard. L. N., Siegmann. W. L., (1969) On the initial value problem for rotating stratified flow, Studies in applied Mathematics, vol. 48, Issue 2, pp. 153-169.
[13]. Piccirillo. P. S., and Van Atta. C. W., (1997) The evolution of a uniformly sheared thermally stratified turbulent flow, Journal of Fluid Mechanics, vol. 334, pp. 61-86.
[14]. Rohr. J. J., Itsweire. E. C., Helland. K. N., Van Atta. C. W., (1988b) An investigation of the growth of turbulence in a uniform mean-shear-flow, Journal of Fluid Mechanics, vol. 187, pp.1-33.
[15]. Gerz. T., Shumann. U., Elghobachi. S., (1989) Direct numerical simulation of stratified homogeneous turbulent shear flow, Journal of Fluid Mechanics, vol. 200, pp.563-594.
[16]. Holt. S. F., Koseff. J. R, Ferziger. J. H., (1992) A numerical study of the evolution and structure of homogeneous stably stratified sheared turbulence, Journal of Fluid Mechanic, vol. 237, pp.499-539.
[17]. Kaltenbach. H. J., (1993) Large-Eddy simulation of flow in a plane, asymmetric diffuser. Annual Research Briefs. Center for Turbulence Research, NASA Ames/Stanford Univ., , pp. 175-184.
[18]. Jacobitz. F. G., Sarkar. S., and Van Atta. C. W., (1997) Direct numerical simulations of turbulence evolution in a uniformly sheared and stably stratified flow. Journal of Fluid Mechanics, vol. 342, pp. 231-261.
[19]. Jacobitz. F. G., and Sarkar. S., (1998) The Effect of non vertical shear on turbulence in a stably Stratified Medium, Physics of Fluids, vol. 10, No.5, pp. 1158-1168.
[20]. Jacobitz.. F., Sarkar. S., (1999) On the shear number effect in stratified shear flow, Theoretical and computational fluid dynamics, vol. 13, pp. 171-188.
[21]. Jacobitz. F. G., and Sarkar. S., (2000) Turbulent Mixing in a Vertically Stably Stratified Fluid with Uniform Horizontal Shear, Flow, Turbulence and Combustion, vol. 63, pp. 343-360.
[22]. Jacobitz. F. G., (2000) Scalar transport and mixing in turbulent stratified shear flow, International Journal of Heat and Fluid flow, vol. 21, pp. 535-541.
[23]. Jacobitz. F. G., (2002) A comparison of the turbulence evolution in a stratified fluid with vertical or horizontal shear, Journal of Turbulence, vol. 3, pp. 1-16.
[24]. Speziale. C. G., Sarkar. S., Gatski. T. B., (1991) Modeling the pressure-strain correlation of turbulence: an invariant dynamical system approach, Journal of Fluid Mechanics, vol. 227, pp. 245-272.
[25]. Speziale. C. G., and. Gatski. T. B., (1997) Analysis and modeling of anisotropies in the dissipation rate of turbulence. Journal Fluid Mechanics, vol. 344, pp. 15-180.
[26]. Takahiro MIURA, Koji MATSUBARA and Atsushi SAKURAI, (2012) Turbulent-Heat-Flux and Temperature-Variance Budgets in a Single-Rib Mounting Channel*, Journal of Thermal Science and Technology, Vol. 7, No. 1, pp. 120-134.
[27]. Fatima MADI AROUS, (2016) Numerical simulation with a Reynolds stress turbulence model of flow and heat transfer in rectangular cavities with different aspect ratios, Journal of Thermal Science and Technology, Vol.11, No.1, pp. 1-13.
[28]. Craft. T. J., Launder. B. E., (1989) A new model for the pressure/scalar-gradient correlation and its application to homogeneous and inhomogeneous free shear flows, Paper 17-1, Proc. Seventh Symposium on Turbulent Shear Flows, Stanford, California.
[29]. Schiestel. R., and Elena. L., (1997) Modeling of anisotropic turbulence in rapid rotation, Aerospace Science and Technology, vol. 1, Issue. 7, pp. 441-451.
[30]. Petterson. A., Reif. B., Ooi. A., and Durbin. P. A., (2000) On stably stratified shear flows subjected to rotation. Center for turbulence Research Proceeding of the Summer Program.
[31]. Speziale. C. G., and Mhuiris. N. M. G., (1989b) On the prediction of equilibrium states in homogeneous turbulence, Journal Fluid Mechanic, vol. 209, pp. 591-615.

[32]. Chebbi. B., Bouzaiane. M. and Lili. T., (2009) Prediction of equilibrium states of kinematic and thermal fields in homogeneous turbulence submitted to the rotation, International Symposium on Convective Heat and Mass Transfer in Sustainable Energy, Vol. 200, pp. 376-379.

[33]. Naffouti. L. T., Bouzaiane. M., Lili. T., (2012) A study of equilibrium states of homogeneous turbulence submitted to an inclined shear, International Journal of Computer Science Engineering, vol.1, No 2, pp. 126-139.

[34]. Kirilli. G., Shatwell. T., (2016) Generalized scaling of seasonal thermal stratification in lakes, Earth-Science Reviews, vol. 161, pp. 179-190.

[35]. Xian-Xiang Li, Rex Britter, Leslie K. Norford, (2016) Effect of stable stratification on dispersion within urban street canyons: A large-eddy simulation. Atmospheric Environment, vol.144, pp. 47-59.

[36]. Gibson. M. M., Launder. B. E., (1978) Ground effects on pressure fluctuations in the atmospheric boundary layer. Journal of Fluid Mechanics 86 (03), pp. 491-511.

[37]. Launder. B. E., Tselepidakis. S. Fu., (1987) Accommodating the effects of high strain rates in the modeling the pressure strain correlation, The University of Manchester of Science and Technology. March T.F.D/87/5/.

[38]. Launder, B. E., Reece, G., and Rodi, W., (1975) Progress in the development of a Reynolds stress closure. Journal Fluid Mechanic, vol. 68, pp. 537-576.

[39]. Speziale. C. G., Sarkar. S., and Gatski, T. B., (1990) Modeling the rapid pressure-strain correlation of turbulence, ICASE Report no 90-5, Contract Nas-18605.

[40]. Speziale. C. G., Gatski. T. B., Mhuiris. N. M. G., (1989a) A critical comparison of turbulence models for homogeneous shear flows in a rotating frame. NASA Contractor Report 181864. ICASE Report No. 89-43.

[41]. Yang Zhiyin, (2015) Large-Eddy simulation: Past, present and the future, Chinese Journal of Aeronautics, vol. 28, pp. 11-24.

[42]. Fu. S., Launder. B. E., and Tselepidakis. D. P., (1987) Accommodating the Effects of High Strain Rates in Modeling the Pressure-Strain Correlation, UMIST Mech. Engng Dept Rep. TFD/87/5.